ADVANCED MATERIALS AND PROCESSING TECHNIQUES FOR STRUCTURAL APPLICATIONS

Paris 7-9 September 1987

Editors T. KHAN,
A. LASALMONIE

Published by
OFFICE NATIONAL D'ETUDES ET DE RECHERCHES AEROSPATIALES
BP 72 - 92322 CHATILLON CEDEX (France)

MECHANISMS OF STRENGTHENING AND OF FRACTURE IN ODS SUPERALLOYS DURING CREEP AND FATIGUE

E. Arzt, D. Elzey and J.H. Schröder

Max-Planck-Institut für Metallforschung,
Institut für Werkstoffwissenschaften,
Seestraße 92, D-7000 Stuttgart 1, FRG

Abstract - Dispersoid particles in oxide-dispersion strengthened (ODS) superalloys do not only increase the creep strength, but also suppress crack initiation during high temperature fatigue. However, irregularities in the grain structure tend to counterbalance these positive dispersoid effects by giving rise to premature material failure. These effects and their mechanisms have been studied in Inconel MA 6000 and MA 754, leading to practical conclusions for improving the mechanical properties of current ODS alloys.

1. INTRODUCTION

Oxide-dispersion strengthened (ODS) superalloys are advanced high-temperature materials which offer considerable advantages over conventional superalloys in demanding applications. They combine good oxidation and corrosion resistance with high creep strength up to a relatively high fraction of their melting points, which predestines them for use in gas turbines, combustion engines and similar applications.

The mechanical high-temperature behaviour of ODS materials is influenced by two microstructural characteristics: (i) a fine dispersion of stable oxide particles which strengthen the alloy at temperatures too high for other mechanisms to contribute, and (ii) an elongated grain structure which is designed to suppress premature intergranular fracture at high temperatures. The detailed mechanisms by which these beneficial effects are achieved have been explored only recently.

In this paper, an account of our present understanding of the mechanisms related to mechanical strength and to fracture in ODS alloys is given. We divide the treatment into two major sections, one devoted to creep, the other to fatigue and creep/fatigue. Emphasis is placed on findings made in the authors' laboratory, while a complete overview of the literature has not been attempted. For a recent review of the processing, structure and properties of ODS superalloys the reader is referred to [1].

2. MECHANISMS OF CREEP STRENGTH AND FRACTURE

Generally, the creep behaviour of ODS materials is greatly improved over their dispersoid-free counterparts when temperatures are high and stresses relatively low. The reason lies in the existence of a "threshold stress" below which creep rates are negligible. Explanations of the threshold stress are therefore essential for the understanding of creep strength in ODS alloys.

The material studied most extensively was the γ'-forming ODS superalloy Inconel MA 6000. In addition to a composition typical of conventional nickel-base superalloys, MA 6000 contains 2.5 vol.-% of incoherent Y_2O_3 dispersoids with an average diameter of 30 nm and a spacing of 160 nm [2,3].

Short-term creep tests under constant compressive loads were carried out at temperatures up to 1050 °C. The applied stresses were about half the Orowan stress of the oxide dispersion. After a test duration of up to 8 h the specimens were cooled under load. The resulting dislocation structures were studied at room and elevated temperature by transmission electron microscopy, mostly under weak-beam conditions [2,4,5]. Great care was exercised to preclude the observation of artefacts.

In addition, crept specimens of MA 6000 were available from a European joint research program (COST 501) for microstructural investigations. In these samples, the evolution of damage and the mechanisms of fracture were studied by means of light microscopy and SEM [6,7].

2.1 Dispersoid-dislocation interaction in creep

Up to 100 examples of dislocation configurations in the vicinity of dispersoids were studied in detail. Invariably, TEM of specimens crept at low stresses and high temperatures revealed an unexpected mechanism by which single lattice dislocations interact with dispersoid particles (fig. 1): The dislocation is held back strongly by the dispersoid although it is almost always observed after it has surmounted the dispersoid by climb. This was also true for in-situ observations at elevated temperatures. These configurations therefore provide strong evidence that the dispersoids do not act as efficient obstacles to dislocation climb, but rather as a "trap", making detachment of the dislocation the decisive event in the deformation process. Hence, dispersoid particles must be considered as exerting an attractive force on dislocations trying to climb over them.

This conclusion is supported by calculations of the interaction forces between a dislocation and an incoherent particle/matrix interface at high temperatures [8]. It is shown that an attractive interaction indeed arises because the dislocation can, by diffusion and sliding of the interface, relax its strain field to a large extent; this leads to a lower energy configuration in the immediate vicinity of the dispersoid. At low temperatures by contrast, this relaxation mechanism is inoperative, and the high modulus of the hard particle leads instead to a repulsion of the dislocation.

Also an attempt has been made to study the dislocation configurations observed by TEM in a more quantitative way. Fig. 2 shows the diameter distribution of the dispersoid particles observed to exert an attractive force on a dislocation, in comparison with the total size distribution of dispersoids in MA 6000. While both distributions match well over the size range, there are indications that dispersoids smaller than about 15 nm do not pin dislocations as effectively as larger dispersoids. The angle subtended by the arms of the dislocation in contact with a dispersoid is another characteristic of the configuration. In TEM foils oriented such that the beam was approximately parallel to the [111] direction, the distribution of these angles was measured (fig. 3). While large angles (up to 160°) have been observed, it is striking that angles smaller than 40° apparently do not occur. In the next section some conclusions regarding the "strength" of attractive dispersoid particles will be drawn from these findings.

2.2 A new model for dispersion-strengthening at high temperatures: "detachment controlled" creep

It is widely accepted that, at high temperatures and low applied stresses, dislocations can circumvent hard particles by climbing over them. If it is assumed that this climb step is rate-controlling (as is done e.g. by Shewfelt and Brown [9]), then some aspects of dispersion-strengthening at high temperatures seem to be in agreement with theoretical predictions: a threshold stress for

dislocation motion is predicted which coincides with those found experimentally, while agreement with the temperature and strain-rate dependence of the strength is usually less accurate. This model, however, relies on a critical assumption concerning the shape of the dislocation in the immediate vicinity of the dispersoid particle: climb is confined to the particle/matrix interface, which leads to sharp dislocation curvatures at the points where it leaves the interface. For particles without an attractive force on dislocations, such a geometry can be ruled out for energetic reasons, see e.g. [10]. Also, if this model were correct, the dislocations should spend most time in climbing up at the particle - much in contrast to the configurations that we have observed by TEM.

The effect of an attractive interaction on the threshold stress for dislocation bypass has been modelled recently [11]. The attraction is incorporated by assigning a lower line tension $T' = k \cdot T$ (where T is the "normal" line tension and $k \leq 1$) to the dislocation segment in (or near) the particle/matrix interface. In terms of the model by Srolovitz et al [8], k is a measure of how far a dislocation can relax its energy near the interface.

The calculations show that, in general, two distinct threshold stresses exist: a threshold for climb, given by

$$\tau_c(k) = 0.4\, k^{5/2}\, \left(\frac{Gb}{\ell}\right) \qquad (1)$$

and a threshold for detachment of the dislocation from the dispersoid:

$$\tau_d = \left[1-k^2\right]^{1/2}\, \left(\frac{Gb}{\ell}\right) \qquad (2)$$

where G is the shear modulus of the matrix material, b the Burgers vector and ℓ the particle spacing. Comparison of these thresholds as a function of k (fig. 4) leads to an important result: if only a small attractive force exists between a dispersoid and a dislocation (corresponding to a dislocation "relaxation" of only about 6 %), the detachment threshold exceeds the climb threshold and detachment becomes the event which controls the strength of the alloy.

Refined calculations show that due to "dipole interactions" of the dislocation arms, the final point of detachment is never reached; this explains the cut-off in angle α (fig. 3b) [2]. Further, the detachment from small particles can be assisted by thermal activation [12]. This has two consequences: (i) the threshold stress practically disappears for particles smaller than about 10 nm, which is in apparent agreement with fig. 2, and (ii) a decrease of the threshold stress with increasing temperature - found in most dispersion-strengthened systems - follows naturally. Both effects are difficult to explain otherwise.

2.3 Damage formation and creep fracture

The full potential of dispersion strengthening can be exploited at high temperatures only if premature failure at grain boundaries transverse to the applied stress is avoided. In an ideal elongated grain structure with a high aspect ratio this weakening effect would be suppressed, and fracture would be transgranular (much like in a single crystal). In current MA 6000, however, recrystallization defects in the form of fine and equiaxed grains are always present. In these locations creep cavities develop easily and coalesce to form an incipient creep crack. These cracks then grow transgranularly till fracture occurs [6,7]. Elimination of these defects would therefore be expected to substantially improve the stress rupture behaviour.

3. MECHANISMS OF HIGH TEMPERATURE FATIGUE

The effects of dispersoids and of grain structure on the high temperature low-cycle fatigue (HTLCF) behaviour of ODS superalloys have not been studied extensively. Our experiments were designed (i) to provide insight into the influence of dispersoids on crack initiation and (ii) to assess the sensitivity to recrystallization defects.

HTLCF experiments were conducted with MA 6000, MA 754 and, for comparison, the dispersoid-free alloy Nimonic 75. Tests have employed triangular waveform cycling (fully reversed), total strain control with and without plastic strain limits, strain rates between 10^{-2} and $10^{-5}\,s^{-1}$ and temperatures ranging from 750 to 1050 °C. Tests conducted until specimen separation or interrupted before separation have then been examined metallographically. Fracture surfaces and polished axial sections were subjected to light- and scanning electron-microscopy (SEM) and separate specimens were prepared for TEM.

3.1 Fracture mechanisms

Several possible mechanisms for the initiation of cracks in MA 6000 during HTLCF have been presented in the literature. Among these mechanisms are cracking at Al-rich spherical inclusions [13], at bubble-like defects [14], and crystallographic Stage I cracking [15]. There are a variety of defects available as potential crack starters, both inclusion-type and as irregularities in the grain structure [6]. LCF studies to date on MA 6000 show that, as is commonly observed for most other metals and alloys, higher test frequencies tend to result in internal crack initiation and lower frequences initiate surface cracks. The influence of temperature on crack initiation has not been studied in detail. However, no clear transition from transgranular to intergranular initiation occurs as is the case for equiaxed-grain alloys.

Figure 5a is a typical fracture surface of a specimen tested to failure in 1500 cycles at 850 °C. Visible are three surface crack initiation sites and one internal site. Closer inspection of the surface initiation sites showed that initiation is not crystallographic but runs very nearly perpendicular to the applied stress and is apparently not associated with inclusion particles. A detail of one of these surface sites is shown in figure 5b, in which a grain boundary may be seen to encircle the point of initiation. These and similar observations indicate that Stage I crack intitiation does not occur under these test conditions. At higher strain amplitudes ($\Delta\epsilon_t \geq 0.45$ %, $N_f \leq 100$), an increasing incidence of slip band formation and crystallographic crack propagation was observed. Slip bands in MA 6000 are usually only rarely observed following HTLCF and apparently require large scale plastic deformation for their formation.

A further detail, seen in figure 6a, allows a closer look at the internal crack initiation. It appears that an inclusion of roughly 100 μm diameter has caused initiation. However, further examination has shown that what appears on the fracture surface as an inclusion is actually the tip of a fine grain. This situation is exemplified in figure 6b, which is an axial section taken from the same specimen but is a crack not related to the fracture surface.

This evidence strongly suggests that the presence of smaller grains is probably the most significant cause of LCF crack initiation in MA 6000 at high temperature.

MA 754 is an ODS version of Ni-20 Cr and exhibits the elongated grain structure common among ODS alloys. Figure 7 is a view of a polished and etched axial section of an MA 754 test sample fatigued 150 cycles at a constant plastic strain amplitude of 0.15 % and a temperature of 750 °C. the slip bands which may be seen in the figure, running at approximately $\pm$ 45° to the stress axis, are very short (3-5 μm) relative to the grain width and occur only infrequently. By comparison, figure 8 shows an axial section of Nimonic 75 fatigued 150 cycles

under the same test conditions. The fine-grained, non-ODS, Ni-20 Cr alloy exhibits uninhibited slip on several systems. The slip bands are tightly yet evenly spaced and extend the entire grain width (d $\approx$ 100 μm). Microcrack formation at twins intersecting the sample surface could be observed whereas the MA 754 showed no evidence of microcracking. These experiments demonstrate that the presence of the oxide dispersion alters the slip character in such a way that Stage I microcrack formation during HTLCF is suppressed. It has been observed that MA 754 is incapable of forming stage I microcracks under these conditions due to slip inhibition by the dispersion [16] although the low stacking fault energy of Ni-20 Cr alloys favours planar deformation.

3.2 Creep-fatigue

A series of so-called 'slow-fast' (S-F) tests were conducted using MA 6000 at 850 °C. Under these test conditions, the specimen is slowly loaded in tension ($\dot{\varepsilon} = 1 \cdot 10^{-5} s^{-1}$) followed by fast loading into compression ($\dot{\varepsilon} = 1 \cdot 10^{-2} s^{-1}$). Results of test conducted to failure under total strain control may be seen in Figure 9 and are compared with 'slow-slow' cycle tests, conducted at a strain rate of $2 \cdot 10^{-5} s^{-1}$. It may be seen that the S-F cyclic lifetimes are 2 to 3 times shorter than correspondig symmetric test lifetimes. Also shown for comparison in figure 9 are results for similar S-F tests conducted by Nazmy [17] using the cast Ni-base alloy IN-738. There is no remarkable difference between MA 6000 and IN-738 under these conditions.

Figure 10 illustrates a typical S-F test fracture surface in which may be seen many individual, internal crack initiation points. Associated with each initiation is a surrounding, radially expanding crack growth front. As may be seen in Figure 11, which is an axial section of this S-F test sample, the cracks initiate intergranularly at the transverse boundaris of low aspect ratio grains. The initiated cracks then extend transgranularly into the surrounding grains.

The crack initiation/growth process occurring under S-F conditions mentioned above, represents an extreme sensitivity to such internal grain structure defects. By comparison, IN-738 initiates surface cracks during S-F cycling [17]. As has been previously reported for other high temperature Ni-base alloys, the S-F cycle has a relatively high rate of damage accumulation [18, 19]. In MA 6000 this is due to intergranular cavitation on the transverse boundaries of small aspect ratio grains during slow tensile loading, which is not reversed during compression. Samples tested under symmetric, slow-slow conditions and interrupted at equivalent cyclic lives showed practically no accumulated pore damage.

3.3. Dislocation configuration

TEM studies of fatigued samples generally revealed a relatively homogeneous distribution of dislocations. Other than occasional networks surrounding γ' particles (fig. 12) no dislocation cell formation or other inhomogeneities in dislocation distribution could be observed (fig. 13). This evidence also suggests that the oxide dispersion in MA 6000 acts to inhibit concentrations of glide dislocations and thus the formation of planar slip bands. Detailed observations of dispersoid-dislocation interactions (fig. 14) suggest that slip inhibition is again due to a resistance to dislocation detachment.

4. CONCLUSIONS

1) The mechanism of dispersion strengthening at high temperatures differs markedly from that at room temperature. Both TEM studies and theoretical analyses suggest that ODS alloys derive their outstanding creep ctrength from a resistance of dislocation detachment from the dispersoid particles. The model presented can explain a dependence of the "threshold stress" on both dispersoid particle size and temperature.

2) The role of the dispersoids during fatigue of ODS alloys consists in the inhibition of planar slip (by a similar dislocation detachment mechanism as in creep) and hence of slip band formation. This leads to suppression of stage I crack initiation.

3) The full potential of dispersion strengthening at high temperature can be exploited only with defect-free elongated grain structures. Recrystallization defects in the form of fine-grained regions are sites of early creep damage formation, leading to premature stress rupture.

4) Recrystallization defects are also extremely detrimental to the HTLCF behaviour. In MA 6000, cracks can initiate at these defects, counter-balancing the positive effect of the dispersoids on crack formation. For this reason the HTLCF strength of MA 6000 is only comparable, and not superior to, its non-ODS counterpart, IN 738. It follows that by eliminating recrystallization defects, a much improved fatigue strength could be expected.

5) The tendency to premature crack initiation in fine-grained regions increases drastically under asymmetric "slow-fast" loading. This effect manifests itself in an enhanced susceptibility to internal crack initiation. The reason for this behaviour is that the cavitation which occurs during slow tensile loading is not fully reversed during fast compression.

Acknowledgements - This work was carried out within the framework of the European collaborative programme COST 501. The authors gratefully acknowledge financial support by the German BMFT (project numbers 01ZY122 and 03ZYK1228).

6. REFERENCES

1. R.F. SINGER and E. ARZT, Structure, Processing and Properties of ODS Alloys, in "High Temperature Alloys for Gas Turbines and Other Applications 1986", W. Betz et al., eds., D. Reidel, Dordrecht, 1986, pp. 97-126.
2. J.H. SCHRÖDER, Electron Microscopic Investigations of the High Temperature Strengthening Mechanisms in an ODS-Superalloy, Ph.D. Thesis, University of Stuttgart, 1987.
3. J.H. SCHRÖDER and E. ARZT, to be published.
4. J.H. SCHRÖDER and E. ARZT, Weak Beam Studies of Dislocation/Dispersoid Interactions in an ODS Superalloy, Scripta Met. 19 (1985) 1129-1134.
5. E. ARZT and J.H. SCHRÖDER, High Temperature Strength of ODS Superalloys due to Dispersoid-Dislocation Interaction, in "High Temperature Alloys for Gas Turbines and Other Applications 1986", W. Betz et al., eds., D. Reidel, Dordrecht, 1986, pp. 1037-1048.
6. H. ZEIZINGER, Damage in an ODS Superalloy due to High Temperature Low Cycle Fatigue and Creep, Ph.D.Thesis, University of Stuttgart, 1986.
7. H. ZEIZINGER and E. ARZT, The Influence of the Grain Aspect Ratio on the Creep Behaviour of the Dispersion Strengthened Superalloy Inconel MA 6000, to be published.
8. D.J. SROLOVITZ, M.J. LUTON, R. PETKOVIC-LUTON, D.M. BARNETT and W.D. NIX, Diffusionally Modified Dislocation-Particle Elastic Interactions, Acta Met. 32 (1984) 1079-1088.
9. R.S.W. SHEWFELT and L.M. BROWN, High Temperature Strength of Dispersion-hardened Single Crystals. II. Theory, Phil. Mag. 4 (1977) 945-962.
10. J. RÖSLER and E. ARZT, The Kinetics of Climb over Hard Particles. I. Climb without attractive particle-dislocation interaction, to be published.
11. E. ARZT and D.S. WILKINSON, Threshold Stresses for Dislocation Climb over Hard Particles: The Effect of an Attractive Interaction, Acta Met. 34 (1986) 1893-1898.
12. E. ARZT and J. RÖSLER, The Kinetics of Climb over Hard Particles. II. Effects of an Attractive Interaction, to be published.

13. P. ADAM, D. FROSCHHAMMER and H. WILHELM, ODS Superalloys: Processing through Joining, ECM and Coating - Report of Material Properties, Final Report COST 501, MTU, München, 1986.
14. A.J. HUIS IN'T VELD, P.M. BRONSVELD and J.M. DE HOSSON, HTLCF Properties of MA 6000, in "High Temperature Alloys for Gas Turbines and Other Applications", W. Betz et al., eds., D. Reidel, Dordrecht 1986, pp. 1049-1056.
15. J. BRESSERS and E. ARZT, High Temperature Low Cycle Fatigue of INCONEL MA 6000, in "High Temperature Alloys for Gas Turbines and Other Applications", W. Betz et al., eds., D. Reidel, Dordrecht 1986, pp. 1067-1080.
16. D. ELZEY, PhD Thesis, Univ. of Stuttgart, to be published.
17. M.Y. NAZMY, High Temperature Low Cycle Fatigue of IN 738 and Application of Strain Range Partitioning, Met. Trans. A 14A (1983) 449-461.
18. B.K. MIN and R. RAJ, Hold-Time Effects in High Temperature Fatigue, Acta Met. 26 (1978) 1007-1022.
19. J. WAREING, Creep-Fatigue Interaction in Austenitic Stainless Steels, Met. Trans. A 8A (1977) 711-721.

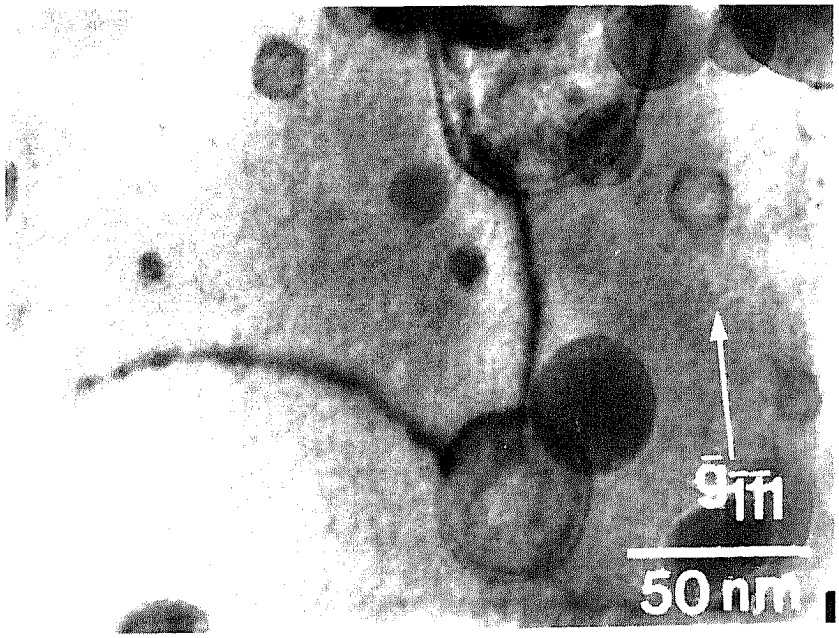

Fig. 1: Typical example of a lattice dislocation interacting with a dispersoid particle during high-temperature creep: strengthening results from an attractive force, making detachment of the dislocation from the dispersoid the decisive event in the deformation process.

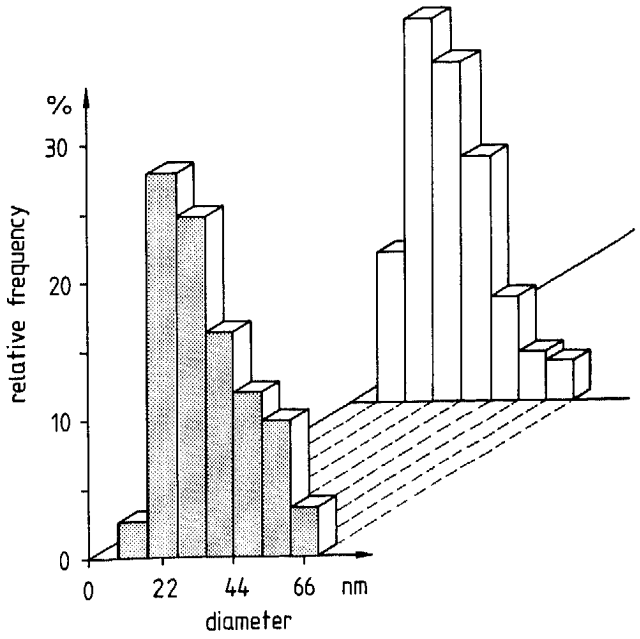

Fig. 2: Diameter distribution of the dispersoid particles observed to exert an attractive force on a dislocation (shaded), in comparison with the total size distribution of dispersoids in MA 6000 (from [2,3]).

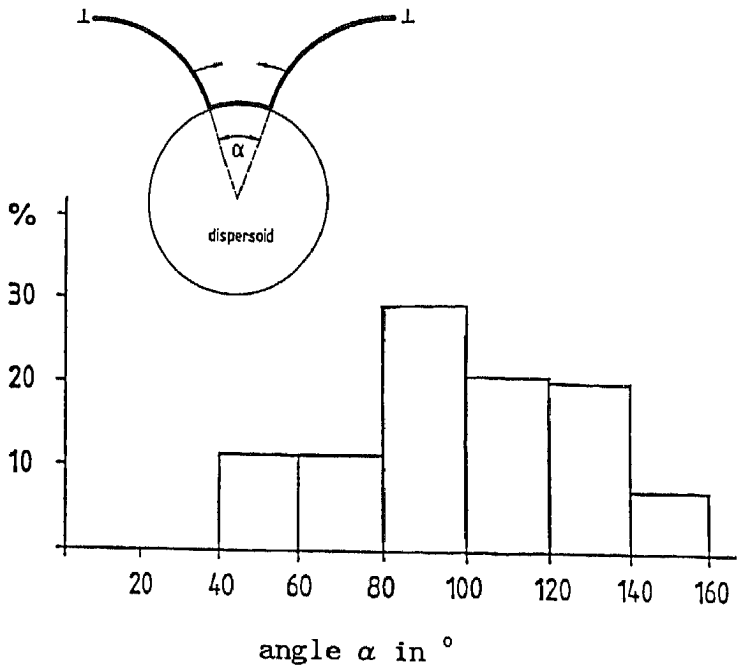

Fig. 3: Distribution of angles α between dislocation arms at dispersoid particles, as measured on TEM micrographs [2,3].

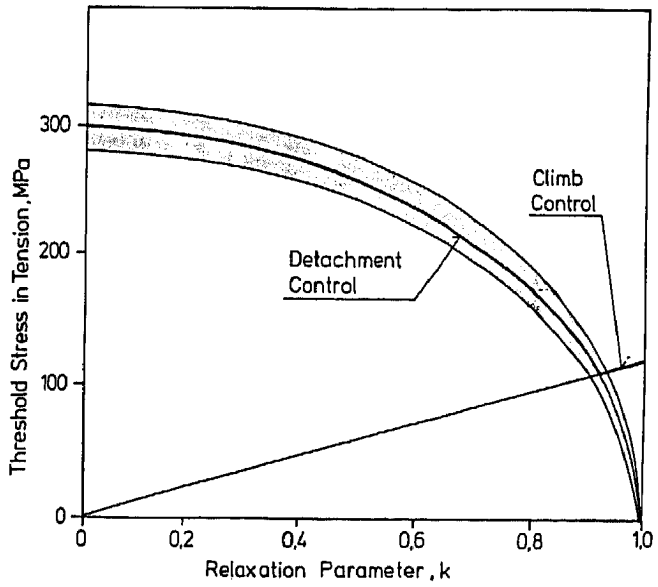

Fig. 4: Threshold stresses due to dislocation climb and to dislocation detachment from attractive particles, as a function of the attraction strength, k (after [11]).

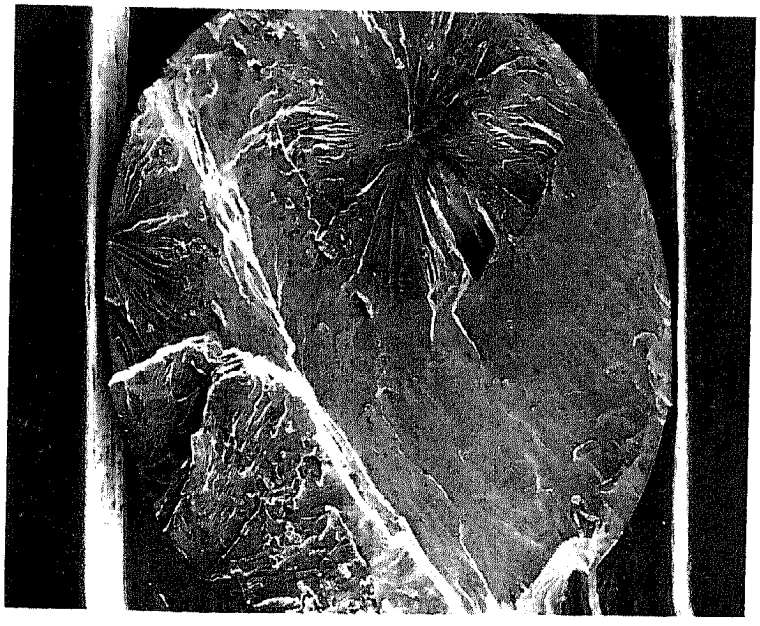

Fig. 5a: MA 6000 fracture showing surface and internal crack initiation. T = 850 °C, $\Delta\epsilon_t/2$ = 0.4 %, $\dot{\epsilon}$ = $1 \cdot 10^{-3}$ [s^{-1}].

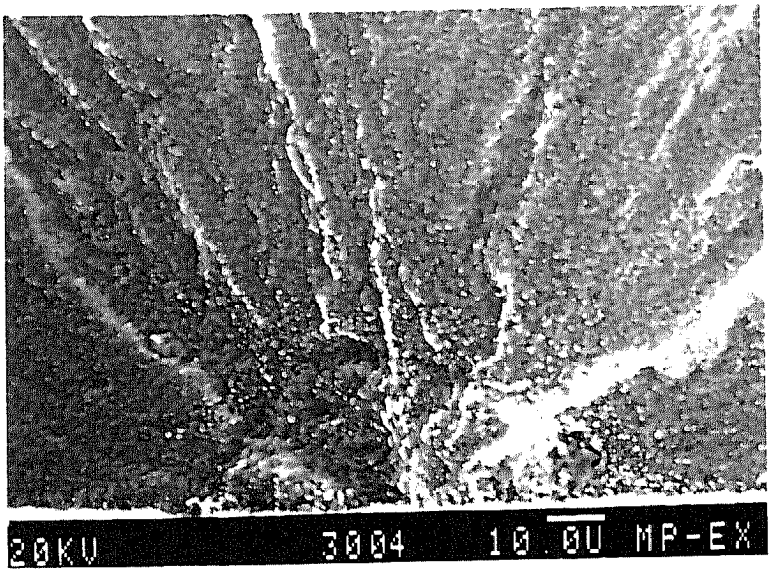

Fig. 5b: Detail of a surface crack initiation site visible in fig. 5a. The outline of a grain boundary may be seen surrounding the initiation point.

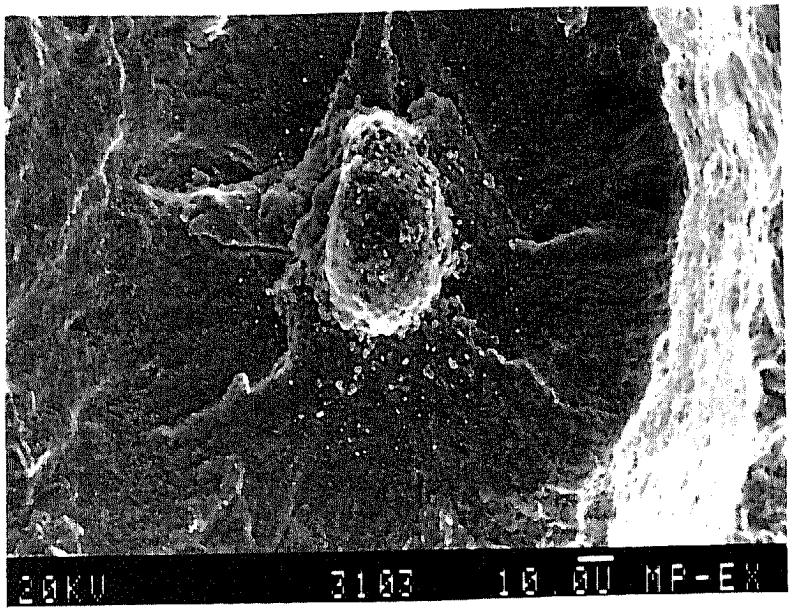

Fig. 6a: A closer look of the internal crack initiation visible in fig. 5a. The apparent inclusion is actually the tip of a fine grain.

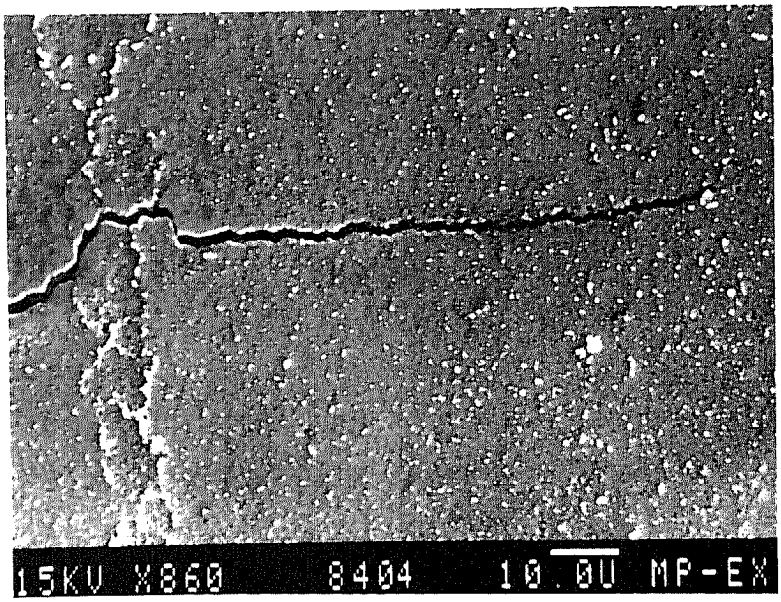

Fig. 6b: Internal crack initiation at fine grains during HTLCF. View is of a polished and etched axial section.

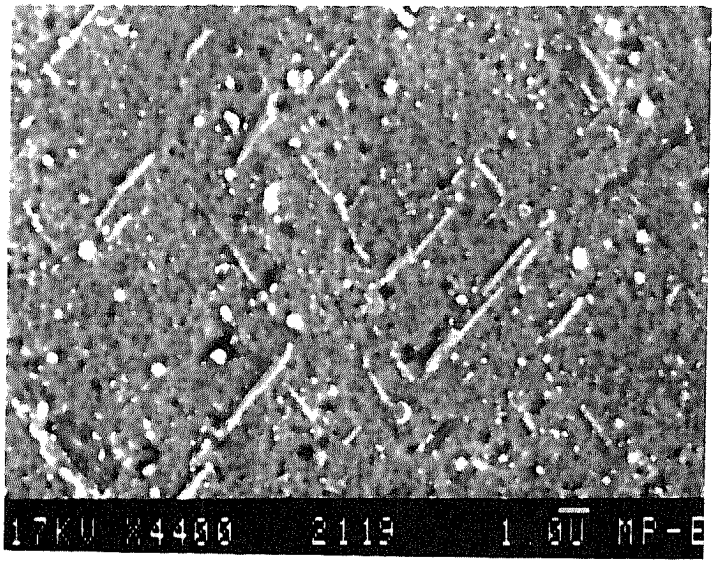

Fig. 7: Short slip band (3-5 μm) in a MA 754 sample tested at 750 °C, inelastic strain amplitude of 0.15 %, interrupted after 150 cycles. Planar slip mode is highly suppressed.

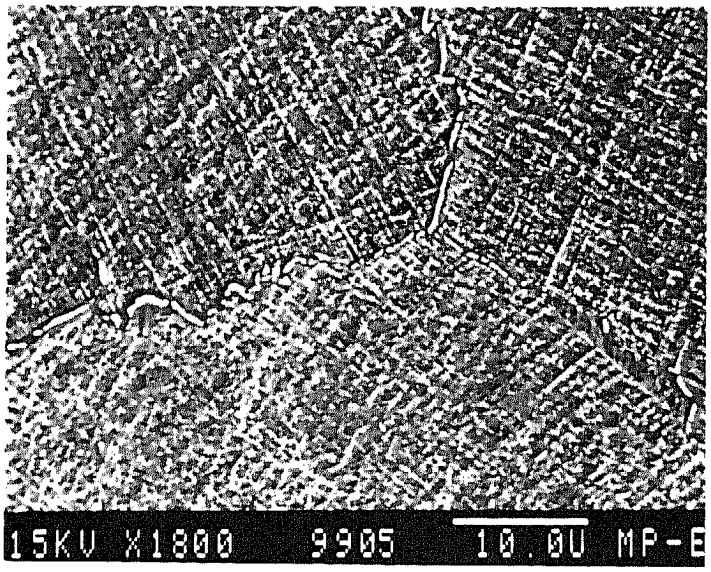

Fig. 8: Slip bands in Nimonic 75, a non-ODS version of MA 754, extend through the entire grain, (d ~ 100 μm). Slip is planar and uninhibited. Same test conditions as for fig. 7.

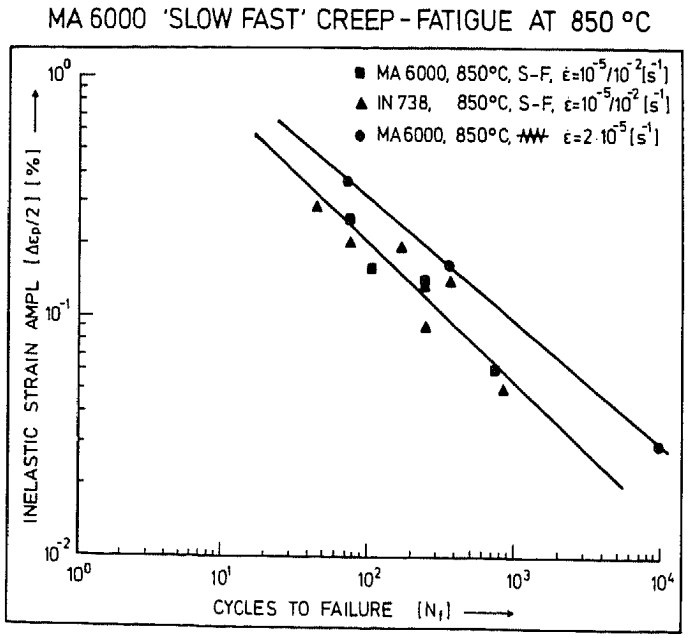

Fig. 9: Results of 'slow-fast' creep-fatigue tests of MA 6000. S-F lifetimes are a factor of 2 to 3 shorter than symmetric cycle tests at the same frequency. S-F results for IN-738 are comparable with those of MA 6000.

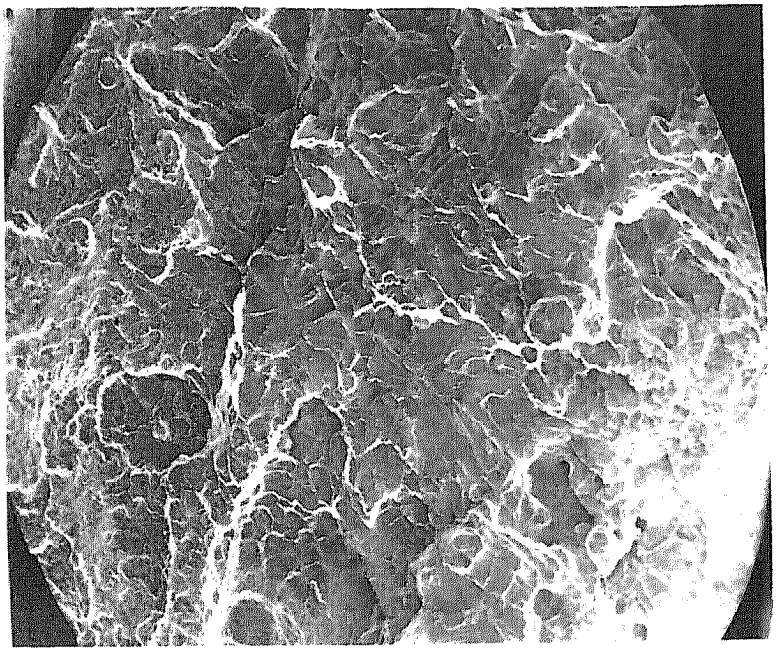

Fig. 10: Fracture surface of an MA 6000 sample tested under 'slow-fast' conditions. At least 27 internal crack initiation points could be identified. T = 850 °C, $\Delta\epsilon_t/2$ = 0.3 %, N_f = 735 cycles.

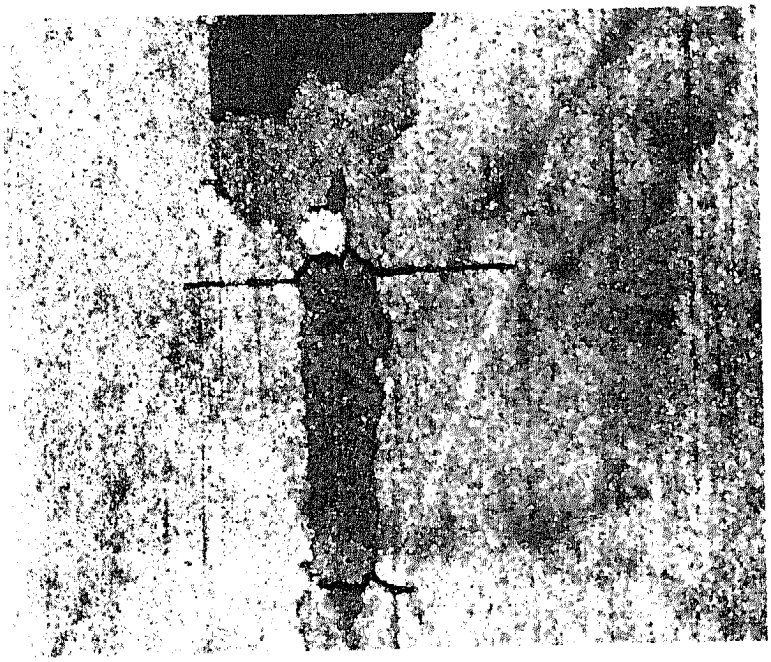

Fig. 11: An axial section of sample shown in fig. 10. Cracks initiate internally on transverse grain boundaries of low aspect ratio grains.

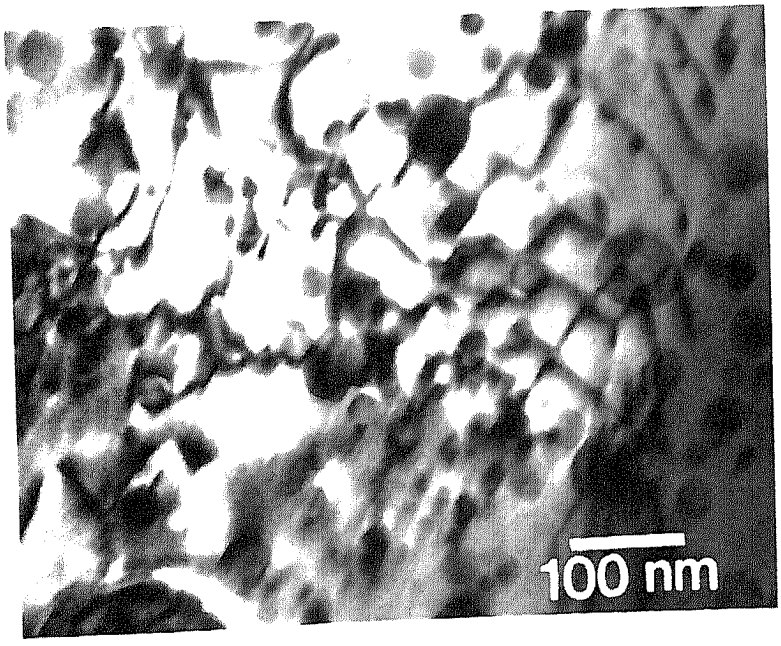

Fig. 12: Dislocation network following 'slow-fast' creep-fatigue at 850 °C, $\Delta\epsilon_t/2$ = 0.4 %, N = 191 cycles.

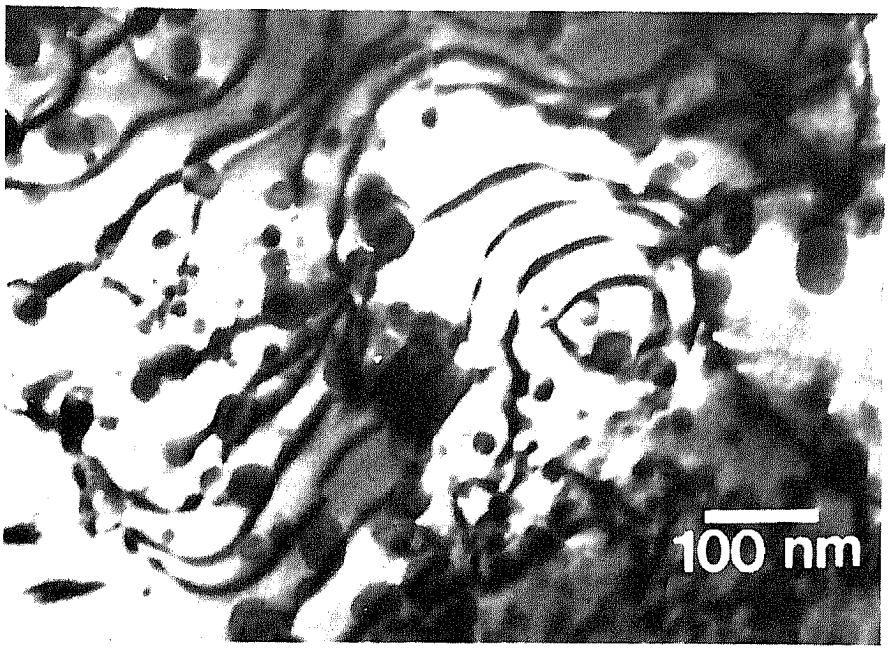

Fig. 13: Typical dislocation distribution following HTLCF at 850 °C, $\Delta\epsilon_t/2$ = 0.4 %, N = 100 cycles.

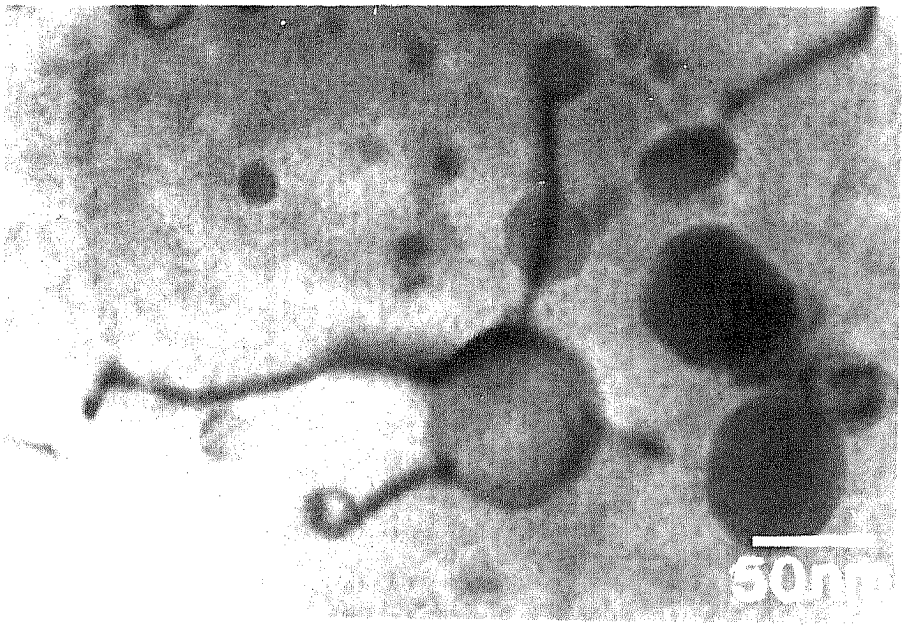

Fig. 14: Dislocation backside-pinning during LCF at 1050 °C.